Monthly Notices
of the
ROYAL ASTRONOMICAL SOCIETY

MNRAS **487,** L13–L17 (2019)
Advance Access publication 2019 May 24

doi:10.1093/mnrasl/slz078

Stopping of porous projectiles in granular targets

María Belén Planes,[1] Emmanuel N. Millán,[2] Herbert M. Urbassek[3]★ and Eduardo M. Bringa[1]

[1]*CONICET and Facultad de Ingenería, Universidad de Mendoza, Mendoza 5500, Argentina*
[2]*CONICET, Facultad de Ciencias Exactas y Naturales and ITIC, Universidad Nacional de Cuyo, Mendoza 5500, Argentina*
[3]*Physics Department and Research Center OPTIMAS, University Kaiserslautern, Erwin-Schrödinger-Straße, D-67663 Kaiserslautern, Germany*

Accepted 2019 May 21. Received 2019 May 16; in original form 2019 March 15

ABSTRACT

Using granular mechanics, we determine the stopping force acting on spherical granular projectiles impinging on a flat granular bed. We find that the stopping force is proportional to the impact energy, as in Poncelet's law. For fixed velocity, it is proportional to the projectile cross-sectional area rather than to its volume. These dependences only hold in the early stages of stopping, before the projectile has been strongly fragmented. Analogies to the stopping of atomic clusters in compact matter are pointed out.

Key words: methods: numerical – planets and satellites: formation – protoplanetary discs.

1 INTRODUCTION

Impacts into granular media have been studied for long; recent reviews are provided by Katsuragi (2016), Omidvar, Iskander & Bless (2014), and in an astrophysical context with a focus on impact cratering by Melosh (1989, 2011). The majority of studies focus on the impact of a hard, rigid impactor – such as a block of rock – on a granular target such as regolith.

Comparatively few studies are concerned with the impacts of projectiles that are granular themselves (Bartali et al. 2013). However, in an astrophysical environment, often the impactor itself is granular and possesses a high porosity. Comets have a higher porosity than previously assumed, reaching values of 72–74 per cent (Kofman et al. 2015; Pätzold et al. 2016), and the same applies to asteroids, which reach porosities of 40–60 per cent (Britt & Consolmagno 2001; Fujiwara et al. 2006). In addition, dust agglomerates, which are ubiquitous in the planetary system, have a high porosity. While their constitution certainly depends on the objects under study, interplanetary dust particles are reported to possess a high variety of porosities with peak values in the range of 0–4 per cent and tails reaching up to >50 per cent (Corrigan et al. 1997). Such dust agglomerates are a frequent source of impacts on other bodies such as moons and asteroids. Impact into regolith in particular occurs frequently on rocky moons and asteroid surfaces (Yamamoto 2002; Nakamura et al. 2013). During the formation of planetary systems, dust aggregates are believed to have filling factors as low as 10^{-4} (Okuzumi et al. 2012; Kataoka et al. 2013; Krijt et al. 2015, 2016).

Granular mechanics offers an important tool to study impacts into granular materials (Dominik & Tielens 1997; Prabhu & Sharp 2005; Paszun & Dominik 2009). Among the first to study such impacts were Tsimring & Volfson (2005) using two-dimensional granular mechanics simulations. Three-dimensional simulations were provided by Hurley, Lim & Andrade (2015), who studied low-velocity impact in granular media with a particular focus on the role of frictional forces. More recently, Li et al. (2016) studied ejecta mass and velocity. Among the few studies considering porous projectiles, Planes et al. (2017) focused on the cratering process.

In this paper, we study impacts of porous aggregates, rather than hard projectiles, on a granular bed. In contrast to previous studies that concentrated on the cratering, fragmentation, and ejection processes, our interest is here with the projectile stopping process, and with the analysis of the stopping force. In particular, we discuss the influence of the projectile size on the slowing-down force of the projectile.

2 METHOD

Both the target and the projectile aggregates are composed of silica grains. All grains are spherical with a radius of $R_{\rm grain} = 0.76$ μm. The target has the form of a cubic box with a side length of 70.7 μm. It contains about 70 000 grains, and has a filling factor of 36 per cent. It was constructed using the method of Ringl, Bringa & Urbassek (2012) by filling grains homogeneously into a box until the required filling factor is reached. We construct spherical projectile aggregates by cutting them out of the target; they hence also have a filling factor of 36 per cent. The number of grains in the projectile, N, varies between 1 and 500.

Initially the projectile is set at a position above the target such that there is no interaction with it. Then the simulation is started by giving each grain in the projectile the same velocity v, which we vary between 5 and 200 m s^{-1}. The top and bottom surfaces of the target are free; at the sides we employ periodic boundary conditions. The time-step of the simulation amounts to 50 ps (Ringl & Urbassek 2012); we perform for each simulation in total 400 000 time-steps,

★ E-mail: urbassek@rhrk.uni-kl.de

amounting to 20 μs. Simulation data are recorded every 0.25 μs. In addition, in some representative simulations, we monitored the output more frequently, every 5 ns, in order to analyse the energy variation in the stopping process with higher resolution.

In several cases we prolonged the simulation time to 10^6 time-steps to verify the convergence of our results. In the last 6×10^5 time steps, the final position varied by less than 8 per cent. In addition, we estimated the statistical error of our simulations by repeating the simulations with a slightly different (lateral) projectile starting position; the differences in the final positions were only 3 per cent.

We employ a granular mechanics simulation code whose details have been published by Ringl & Urbassek (2012). Besides the Hertzian elastic contact forces, it includes intergranular adhesion, viscoelastic energy dissipation as well as friction during sliding, rolling, and twisting motion (Dominik & Tielens 1997). In our simulations we employ the material parameters for silica; the Young's modulus is $Y = 54$ GPa, the Poisson ratio $\nu = 0.17$, and the specific surface energy $\gamma = 25\,\mathrm{mJ\,m^{-2}}$ (Chokshi, Tielens & Hollenbach 1993). The mass density is taken as $\rho = 2 \times 10^3\,\mathrm{kg\,m^{-3}}$ (Blum & Schräpler 2004), such that the mass of a grain amounts to $m = 3.68 \times 10^{-15}$ kg.

Data analysis and rendering of granular snapshots has been performed using OVITO (Stukowski 2010).

3 RESULTS

3.1 A representative case

Fig. 1 demonstrates the penetration of a projectile aggregate into the target for a representative case, $N = 200$ at $v = 50\,\mathrm{m\,s^{-1}}$. Immediately upon impact, the projectile is flattened, assuming a lenslike form at 0.65 μs. After 1.5 μs, the projectile has been fragmented; it covers the bottom of the crater that it has excavated as a thin and non-continuous layer.

Due to the stopping process, energy is transferred from the projectile to the target grains. Fig. 1(b) shows that a considerable volume below and also at the sides of the forming crater has received energy. The volume has reached its maximum between times of 0.65 and 1.3 μs. Later, dissipation by friction forces as well as viscoelastic dissipation reduces the energy again, first at the sides and then below the crater, such that grain motion dies out. A few grains ($\simeq$160) are ejected from the surface in this event. During the expansion phase of the crater, $t \leq 1.5$ μs, the boundary between energized and uncollided target grains is sharp; afterwards, during the cooling phase, energy gradients become softer.

3.2 Stopping force

Fig. 2 shows the decrease of the projectile kinetic energy E with penetration depth z for two velocities and various projectile sizes. Here E has been calculated as the sum of the kinetic energies of all projectile grains, while z denotes the centre-of-mass position of the aggregate. The curves do not start at the initial projectile energy, $E = E_0$, since when the projectile centre of mass enters the target, $z = 0$, half the projectile has already penetrated the target and stopping has already started. We observe an exponential decrease of the energy with z during the initial part of the trajectory; the higher the velocity, the longer the exponential decrease continues. After the end of the exponential phase, the kinetic energy quickly drops to zero; we correlate this abrupt decay with the aggregate fragmentation occurring at the end of the trajectory. The decay length of the exponential phase depends on the projectile size N; larger aggregates have a longer decay length.

It might be surmised that the transition from the exponential regime to the final abrupt-stopping regime occurs at a fixed energy value, $E_{\min}$, which is independent of E_0. However, inspection of our data (not shown here) excludes this possibility.

Denoting the decay length of the projectile energy by λ and the initial projectile energy by E_0, the results of Fig. 2 can be quantified as

$$E = E_0 e^{-z/\lambda}. \tag{1}$$

An essential result of our data analysis is that λ depends only on the projectile size N, but not on the projectile energy or velocity, $\lambda = \lambda(N)$.

Such a law, equation (1), corresponds to an energy-proportional stopping power (or 'stopping force'; Sigmund 2000) of the cluster. The stopping force, $\mathrm{d}E/\mathrm{d}z$ is generally defined as the energy lost, $\mathrm{d}E$, while traversing a small path length, $\mathrm{d}z$. It is equal to the force F decelerating the projectile, since

$$\frac{\mathrm{d}E}{\mathrm{d}z} = Mv\frac{\mathrm{d}v}{\mathrm{d}z} = M\frac{\mathrm{d}v}{\mathrm{d}t} = F. \tag{2}$$

Here, the projectile mass, $M = Nm$, and the projectile velocity v have been used; the last identity simply expresses Newton's second law. In granular mechanics, the stopping force is often denoted as the 'drag force'.

For energy-proportional stopping,

$$\frac{\mathrm{d}E}{\mathrm{d}z} = -\frac{E}{\lambda}, \tag{3}$$

the decrease of E with z indeed follows the law, equation (1), observed by us. Such a law is known in the literature as Poncelet's law (due to its use in the stopping of rigid solids in granular matter) or as the inertial drag (Katsuragi & Durian 2007; Omidvar et al. 2014; Katsuragi 2016).

Our simulations allow us to extract the value of λ and its size dependence. We extract it from the slopes of the $E(z)$ dependences such as those displayed in Fig. 2. The results are displayed in Fig. 3; for clarity, we restrict the figure to two velocities, 25 and 50 $\mathrm{m\,s^{-1}}$. We see that λ is indeed independent of the projectile velocity; its dependence on projectile size follows a power law

$$\lambda = \lambda_1 N^{\alpha}, \tag{4}$$

where $\alpha \simeq 0.335$, close to 1/3. The length λ_1 quantifies the stopping of a monomer; it has a value of 0.78 μm.

The fact that the decay length increases – and hence stopping decreases – with projectile size is a prime result of this study. This behaviour is analogous to that found for atomic cluster impact into bulk materials (Anders & Urbassek 2007; Anders et al. 2011). There, for such diverse systems as Cu cluster impact into a Cu target, Ar cluster impact into a condensed Ar target, and even Au cluster impact into condensed Ar targets, molecular dynamics simulations exhibit an energy-proportional stopping with a pre-factor that depends on projectile size as a power law, with an exponent of around 1/3. The same exponent was also found in experiments and simulations of Ag cluster impacts into graphite (Carroll et al. 2000; Pratontep et al. 2003). The fact that we find (approximately) the same size dependence here points to a common physical origin of this dependence.

The idea leading to an increase of the decay length λ as a power law, equation (4), with $\alpha \simeq 1/3$ may be expressed as follows. A *size-independent* coefficient λ in the stopping force, equation (1), would

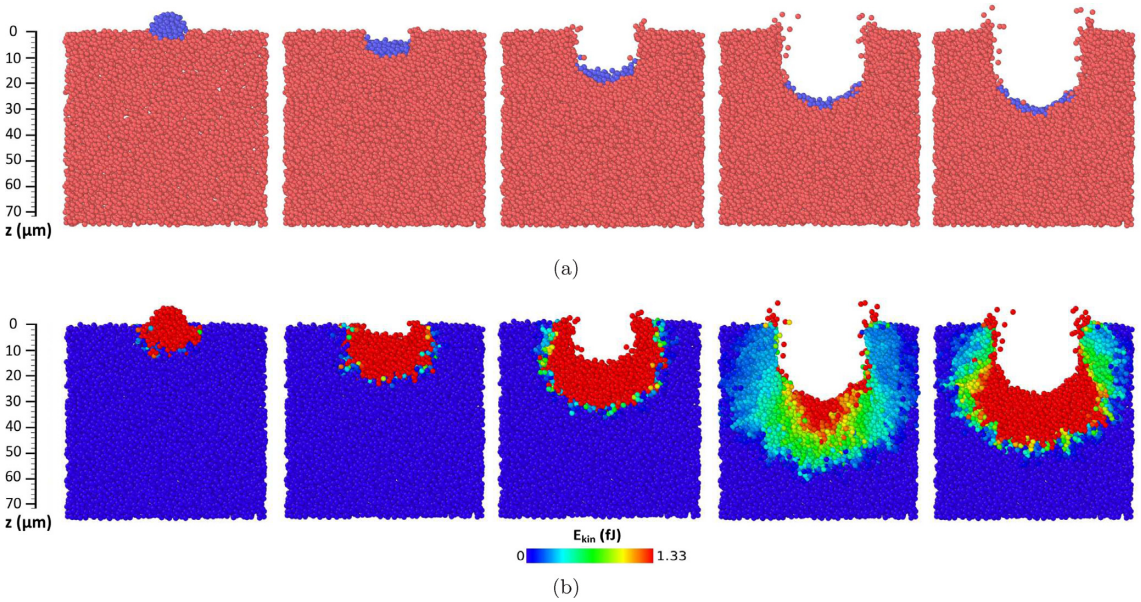

Figure 1. Time series of snapshots showing the stopping of an aggregate of $N = 200$ grains impacting with a velocity of $v = 50\,\mathrm{m\,s^{-1}}$ on a flat granular bed. Times are chosen as (from left to right) 0.325, 0.65, 1.5, 3.75, and 5 μs. Grains are coloured according to (a) grain origin (blue: projectile, red: target); (b) grain kinetic energy in fJ. Slices shown are 6 μm thick.

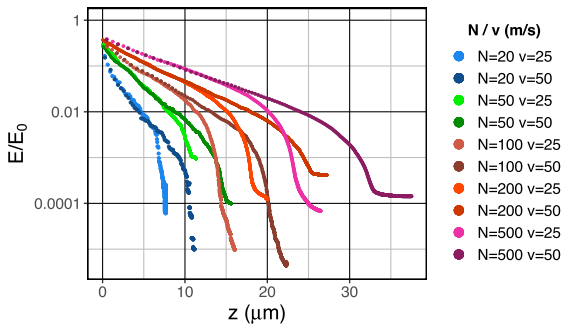

Figure 2. Decrease of the normalized aggregate kinetic energy, E/E_0, as a function of the penetration depth, z, for aggregates with various sizes, N, and velocities, v.

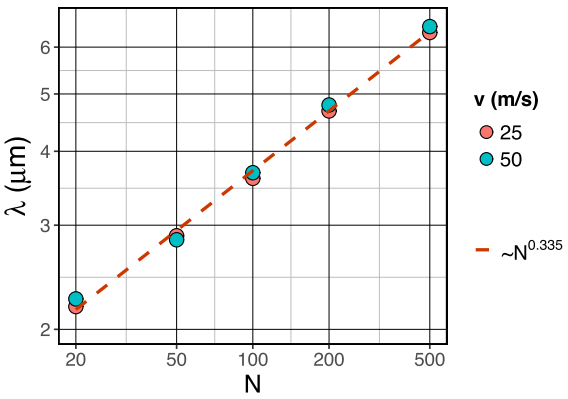

Figure 3. Variation of λ, equation (1), with N for velocities $v = 25$ and $50\,\mathrm{m\,s^{-1}}$. The results demonstrate that λ is independent of v and depends on N as a power law, equation (4).

mean that each grain in the aggregate experiences the same stopping, and this stopping is independent of the other grains surrounding it. Writing $E_\mathrm{g} = E/N$ for the energy of a grain in the projectile, we can rewrite equation (3) as

$$\frac{\mathrm{d}E}{\mathrm{d}z} = -N\frac{E_\mathrm{g}}{\lambda_1}. \tag{5}$$

Under this assumption, the stopping of equi-velocity aggregates increases in proportion to the number of grains in the aggregate.

If however the stopping is proportional to the *cross-sectional area* rather than to the projectile volume, it is

$$\frac{\mathrm{d}E}{\mathrm{d}z} = -N^{2/3}\frac{E_\mathrm{g}}{\lambda_1}. \tag{6}$$

This law is identical with equations (3) and (4) with $\alpha = 1/3$ (Carroll et al. 2000; Anders & Urbassek 2005).

The idea that the stopping force of equi-velocity clusters decreases with increasing cluster size has first been known under the notion of the 'clearing-the-way effect' (Sigmund 1989; Shulga, Vicanek & Sigmund 1989); this term puts emphasis on the fact that the front grains in the projectile suffer the heaviest collisions with the target while the following grains encounter matter that has either been removed from the projectile path or at least has a reduced relative velocity, thus effectively diminishing the stopping force.

We finally note that an inertial drag term proportional to v^2 and proportional to the cross-sectional area of the projectile can be calculated from the macroscopic hydrodynamics at large Reynolds numbers, i.e. when viscous effects are small (see e.g. chapter 2.6.2, Katsuragi 2016).

3.3 Range and stopping time

Under an energy-proportional stopping, equation (3), projectiles never come to rest, while their energy decreases exponentially with distance to the surface (cf. equation 1 and Fig. 1). Indeed, denoting as the projectile range the depth $Z(\epsilon)$, where the projectile energy

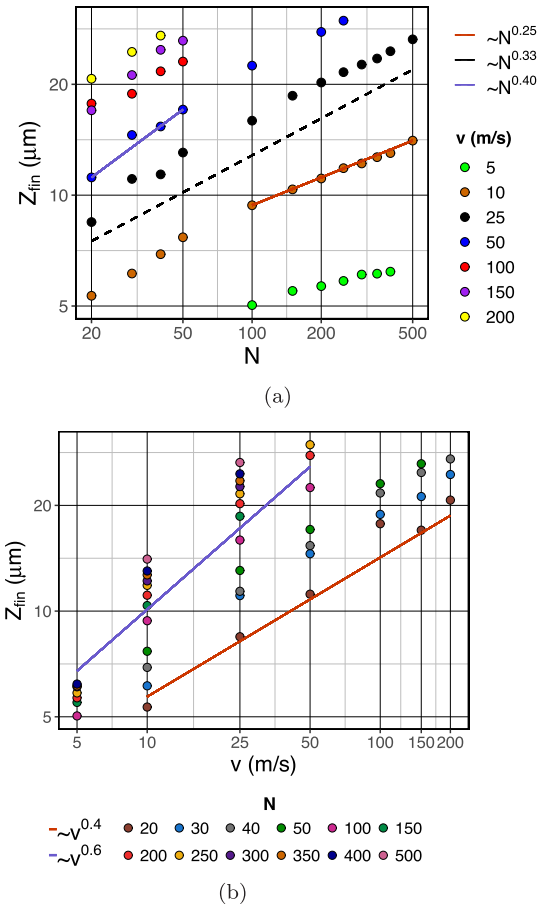

Figure 4. Dependence of the total aggregate penetration depth, $Z_{\rm fin}$, on the (a) aggregate size N for various aggregate velocities v and (b) aggregate velocity v for various aggregate sizes N.

has decreased to a fraction, ϵ, of the initial energy, we have

$$Z(\epsilon) = \lambda \ln \frac{1}{\epsilon} \tag{7}$$

in the energy-proportional stopping regime, expressing the formally infinite range as $\epsilon \to 0$.

However, as noted above, the stopping force becomes stronger as soon as projectile fragmentation sets in (see Fig. 2), leading to a finite value of the actual range, $Z_{\rm fin}$. We plot in Fig. 4 the dependence of the penetration depth $Z_{\rm fin}$ on the projectile size and the velocity. Indeed the size dependence of $Z_{\rm fin}$, Fig. 4(a), follows well the $N^{1/3}$ dependence of the stopping discussed above, even though the data now refer to the complete stopping of the projectile beyond the validity of the exponential regime. This is in accordance with the observed dependence for atomistic impacts of different materials (Popok et al. 2011).

However, the velocity dependence, Fig. 4(b), of $Z_{\rm fin}$ differs strongly from that expected from equation (7), which predicts $Z(\epsilon)$ to be independent of velocity. Rather we find that $Z_{\rm fin}$ exhibits a pronounced velocity dependence that follows a power law, $Z_{\rm fin} \propto v^{\beta}$, with $\beta = 0.4$–0.6. Indeed the power seems to increase slightly with projectile size, N. The origin of the velocity dependence of $Z_{\rm fin}$ – in contrast to $Z(\epsilon)$ – is easy to spot: The exponential stopping regime ends earlier for slow particles than for fast particles (see Fig. 2); since projectiles are stopped quickly once they leave the exponential regime, the finite range of validity of the exponential

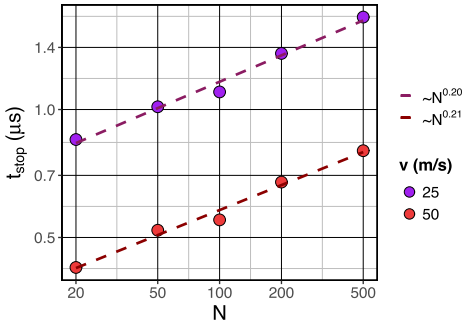

Figure 5. Dependence of the stopping time, $t_{\rm stop}$, on the aggregate size, N, for velocities $v = 25$ and $50\,{\rm m\,s^{-1}}$.

stopping regime introduces a strong velocity dependence into the actual range, $Z_{\rm fin}$.

The exponent β can be discussed in the light of available studies on the penetration depth of rigid impactors (Ambroso et al. 2005) and of the resulting crater sizes (Melosh 1989; Holsapple 1993; Katsuragi 2016). There, a proportionality with $E_0^{1/3}$ (corresponding to $\beta = 0.67$) is interpreted as a strength-dominated behaviour, where energy is dissipated by displacing all particles in the crater volume. A weaker dependence, $E_0^{1/4}$ ($\beta = 0.5$), is described as the gravity-dominated regime, as here also work against the gravitational field costs energy. Our results lie on the lower side of this window of β values, indicating that besides material strength other energy dissipation channels, such as intergranular friction, are operative.

Finally, we may discuss the time, $t_{\rm stop}$, that it takes for the aggregate to slow down. Using Newton's law, equation (2), and the energy-proportional stopping, equation (3), we have

$$M\frac{{\rm d}v}{{\rm d}t} = -\frac{M}{2}\frac{1}{\lambda}v^2. \tag{8}$$

This equation can be trivially integrated to find the time $t_{\rm stop}$ at which the projectile velocity decreased from its initial value v to a fraction $\sqrt{\epsilon}v$,

$$t_{\rm stop} = \frac{2\lambda}{v}\left[\frac{1}{\sqrt{\epsilon}} - 1\right]. \tag{9}$$

Hence, $t_{\rm stop} \simeq \lambda/v$, up to a factor of order unity. Again, for $\epsilon \to 0$, the stopping time formally diverges.

We plot in Fig. 5 the time it takes projectiles to slow down to a fraction, $\epsilon = 0.1$, of the initial energy. Indeed, the data show an approximate $N^{1/3}$ dependence of $t_{\rm stop}$ as it originates from the proportionality of $t_{\rm stop}$ with λ. Also the $1/v$ dependence is manifest, in that aggregates with $v = 50\,{\rm m\,s^{-1}}$ need only half the time for stopping as compared to aggregates with $v = 25\,{\rm m\,s^{-1}}$.

4 SUMMARY

We identified a regime in the stopping of granular aggregates in which the projectile kinetic energy decreases exponentially with penetration depth. This regime ends when the projectile is so strongly fragmented that individual grains are stopped in the target rather than the aggregate as an ensemble. The stopping processes occurring during and after projectile fragmentation are complex, since they are influenced by fragment shape and even fragment–fragment collisions can occur; also energy dissipation processes resulting from intergranular friction and viscoelastic forces become more dominant at small grain velocities. We therefore exclude them from our analysis.

We have assumed equally weak bonding amongst grains in the projectile and in the target. Changing this scenario might lead to different results. A projectile with weaker bonding than the target will likely fragment completely upon impact, and strongly bonding the projectile will approach the limit of a compact impactor. Our results indicate that, even in this regime of weak bonding, stopping can be described using Poncelet's law, which was originally designed for the stopping of compact objects in granular media (Katsuragi & Durian 2007). This regime is characterized by a stopping force proportional to the projectile energy. In our simulations, this stopping phase proceeds extremely rapidly and, therefore, most of the energy is lost while the projectile maintains its integrity, and fragmentation can be roughly neglected.

In addition, the stopping force of an aggregate containing N grains is proportional to $N^{2/3}$ rather than N; that is, it increases with the cross-sectional area rather than with the volume of the projectile. Such a dependence is reminiscent of hydrodynamic drag forces, but has also been found in the stopping of (compact) atomic clusters in bulk materials. The grains at the collision interface lose energy while the grains farther up in the projectile are not yet aware of that energy loss, until nearly complete cluster fragmentation occurs: the 'clearing the way effect' (Anders & Urbassek 2007).

These results are relevant for the interaction of granular aggregates impinging on porous matter with applications in dust interaction with rocky moons or asteroids, mass-asymmetric collisions of dust aggregates in the protoplanetary disc, and collisions between particles in planetary rings. For instance, this might be relevant for mixing in regoliths like the lunar regolith (Szalay et al. 2019).

ACKNOWLEDGEMENTS

We thank for useful discussions with S. Simondi and N. Arista. ENM acknowledges support by a SIIP-UNCuyo grant and EMB thanks PICT2014-0696.

REFERENCES

Ambroso M. A., Santore C. R., Abate A. R., Durian D. J., 2005, Phys. Rev. E, 71, 051305
Anders C., Urbassek H. M., 2005, Nucl. Instrum. Meth. B, 228, 57
Anders C., Urbassek H. M., 2007, Nucl. Instrum. Meth. B, 258, 497
Anders C., Bringa E. M., Ziegenhain G., Urbassek H. M., 2011, New J. Phys., 13, 113019
Bartali R., Rodriguez-Linan G. M., Nahmad-Molinari Y., Sarocchi D., 2013, Role of the Granular Nature of Meteoritic Projectiles in Impact Crater Morphogenesis. preprint (arXiv:1302.0259v2)
Blum J., Schräpler R., 2004, Phys. Rev. Lett., 93, 115503
Britt D. T., Consolmagno G. J., 2001, Icarus, 152, 134
Carroll S. J., Nellist P. D., Palmer R. E., Hobday S., Smith R., 2000, Phys. Rev. Lett., 84, 2654
Chokshi A., Tielens A. G. G. M., Hollenbach D., 1993, ApJ, 407, 806
Corrigan C. M., Zolensky M. E., Dahl J., Long M., Weir J., Sapp C., Burkett P. J., 1997, Meteorit. Planet. Sci., 32, 509
Dominik C., Tielens A. G. G. M., 1997, ApJ, 480, 647
Fujiwara A. et al., 2006, Science, 312, 1330
Holsapple K. A., 1993, Annu. Rev. Earth Planet. Sci., 21, 333
Hurley R. C., Lim K.-W., Andrade J. E., 2015, in Iskander M., Bless S., Omidvar M., eds, Rapid Penetration into Granular Media. Elsevier, Oxford, p. 291
Kataoka A., Tanaka H., Okuzumi S., Wada K., 2013, A&A, 557, L4
Katsuragi H., 2016, Physics of Soft Impact and Cratering. Lecture Notes in Physics, Vol. 910. Springer, Tokyo, Japan
Katsuragi H., Durian D. J., 2007, Nature Phys., 3, 420
Kofman W. et al., 2015, Science, 349, aab0639
Krijt S., Ormel C. W., Dominik C., Tielens A. G. G. M., 2015, A&A, 574, A83
Krijt S., Ormel C. W., Dominik C., Tielens A. G. G. M., 2016, A&A, 586, A20
Li Y., Dove A., Curtis J. S., Colwell J. E., 2016, Powder Technol., 288, 303
Melosh H. J., 1989, Impact Cratering: A Geologic Process. Oxford Univ. Press, New York
Melosh H. J., 2011, Planetary Surface Processes. Cambridge Univ. Press, Cambridge
Nakamura A. M., Setoh M., Wada K., Yamashita Y., Sangen K., 2013, Icarus, 223, 222
Okuzumi S., Tanaka H., Kobayashi H., Wada K., 2012, ApJ, 752, 106
Omidvar M., Iskander M., Bless S., 2014, Int. J. Impact Eng., 66, 60
Paszun D., Dominik C., 2009, A&A, 507, 1023
Pätzold M. et al., 2016, Nature, 530, 63
Planes M. B., Millán E. N., Urbassek H. M., Bringa E. M., 2017, A&A, 607, A19
Popok V. N., Barke I., Campbell E. E. B., Meiwes-Broer K.-H., 2011, Surf. Sci. Rep., 66, 347
Prabhu N. V., Sharp K. A., 2005, Annu. Rev. Phys. Chem., 56, 521
Pratontep S., Preece P., Xirouchaki C., Palmer R. E., Sanz-Navarro C. F., Kenny S. D., Smith R., 2003, Phys. Rev. Lett., 90, 055503
Ringl C., Urbassek H. M., 2012, Comput. Phys. Commun., 183, 986
Ringl C., Bringa E. M., Urbassek H. M., 2012, Phys. Rev. E, 86, 061313
Shulga V. I., Vicanek M., Sigmund P., 1989, Phys. Rev. A, 39, 3360
Sigmund P., 1989, J. Vac. Sci. Technol., A7, 585
Sigmund P., 2000, ICRU News, 1, 5
Stukowski A., 2010, Model. Simul. Mater. Sci. Eng., 18, 015012
Szalay J. R., Pokorny P., Sternovsky Z., Kupihar Z., Poppe A. R., Horanyi M., 2019, J. Geophys. Res., 124, 143
Tsimring L. S., Volfson D., 2005, in Garcia-Rojo R., Herrmann H. J., McNamara S., eds, Powders and Grains 2005. A. A. Balkema, Rotterdam, p. 1215
Yamamoto S., 2002, Icarus, 158, 87

This paper has been typeset from a TEX/LATEX file prepared by the author.